PHYSICAL REVIEW B VOLUME 27, NUMBER 7 1 APRIL 1983

Theory of double electron-muon resonance

T. L. Estle and D. A. Vanderwater*
Rice University, Houston, Texas 77251
(Received 4 October 1982)

The theory of double electron-muon resonance is developed and particularized to the case of muonium and of the anomalous muonium center observed in silicon, germanium, and diamond. The theory can be used to explain and analyze the coherence effects observed in muon-spin—rotation frequency spectra resulting from intense near-resonant rf fields. The technique can, in principle, be used to observe EPR transitions which are otherwise unobservable by muon-spin rotation.

I. INTRODUCTION

During the last few years a growing number of studies have been made using a technique known as muon-spin rotation (or μSR).[1,2] Muon-spin rotation is a form of magnetic resonance of muons, usually μ^+, which are implanted in solids. In this paper we describe the theory of double electron-muon resonance (DEMUR), a variation of μSR in which an intense rf magnetic field drives the coupled-spin system of a muoniumlike center.[3]

When a beam of spin-polarized positive muons strikes a solid target, the muons stop and thermalize quickly with virtually no lost polarization.[2] The muon spins then precess in the effective local fields and ultimately the muons decay with a lifetime of 2.2. μsec. In the weak decay of the muon a positron is emitted preferentially along the direction of the μ^+ spin.[2] These decay positrons are used to detect μSR.

Therefore, muon-spin rotation is a form of free-precession magnetic resonance. By Fourier transformation of the time-differential positron histograms obtained from a large number of muons the frequencies and amplitudes of the components of the precession of the μ^+ spin polarization can be obtained. The μSR frequency spectrum of muonium or muoniumlike centers (an electron spin of $\frac{1}{2}$ coupled to the μ^+ spin, also $\frac{1}{2}$) gives the frequencies of the allowed magnetic dipole transitions of the μ^+ spin. The information obtained is similar to the information obtained by electron nuclear double resonance (ENDOR) of paramagnetic centers. However, the allowed magnetic dipole transitions of the electron spin may be unobservably weak in the μSR frequency spectrum. In that case μSR will not provide much information of the sort obtainable from electron paramagnetic resonance (EPR), such as the electronic g factor.

In contrast to μSR, DEMUR permits observation of EPR transitions even when they are not directly observable as lines in the μSR frequency spectrum. In DEMUR magnetic dipole transitions of the electron spin are driven coherently with an applied rf magnetic field and the resultant structure in the μSR frequency spectrum is used to detect the electron paramagnetic resonance.

The first DEMUR experiment was performed on muonium in quartz and, to date, this is the only system studied.[4,5] For muonium in low fields there are two frequencies in the μSR spectrum, the $\Delta M_F = \pm 1$ transitions within the $F=1$ triplet. These are also allowed magnetic dipole transitions for the electron spin. Driving either of these two transitions produces characteristic splittings of both frequency components in the μSR spectrum demonstrating the essential correctness of the theory and illustrating one application of the technique. The coherence effects observed in this way were particularly striking.[4,5]

To illustrate how this structure appears for a simple example consider a spin-$\frac{1}{2}$ system. Quite generally, if the magnetic resonance transition for a spin of $\frac{1}{2}$ is driven coherently, then there are three precessional frequencies for the component of the spin transverse to the static magnetic field rather than the single frequency obtained in free precession. These three frequencies are the rf frequency and two symmetrically-placed side bands. The splitting with the applied frequency exactly on resonance is the Larmor frequency in a field equal to the transverse component of the rf field rotating in the same sense as the spin precesses. (This is sometimes referred to as the Rabi frequency.) The component of the spin polarization parallel to the static magnetic field has a static part and a term oscillating at a frequency equal to the frequency splitting of the transverse component. (In this we have ignored the com-

ponent of the rf field which rotates in the opposite sense to the precession of the spin.)

In DEMUR, if the frequencies of the transitions are well separated, then choosing an rf frequency close to one transition will split that frequency into three just as for the spin-$\frac{1}{2}$ case. The middle frequency is the rf frequency and the splitting of the side bands on resonance is approximately equal to the Larmor frequency of the electron spin in the transverse component of the properly rotating component of the rf magnetic field. If a particular μSR frequency arises from a transition with only one of the two states in common with the transition being driven, then that frequency is split into two with the same splitting as for the driven transition. Both of these effects were observed in the experiment on muonium in quartz.[4,5] If the driven transition and the μSR "transition" have no common end states, then that part of the μSR frequency spectrum is unchanged by the rf field. Also there is a dc component to the μ^+ spin polarization and a low-frequency component oscillating at a frequency equal to the frequency splitting of the high-frequency lines. These components are parallel to the static field.

For muonium in quartz[4-6] and the muoniumlike centers in group-IV elemental semiconductors[7,8] the observed linewidths under many conditions are instrumental and relaxation can be neglected. Thus we have described DEMUR theoretically by solving the coupled differential equations for the coefficients of the stationary-state wave functions in the general time-dependent wave function, neglecting relaxation and making appropriate approximations. The time-dependent wave function, written in terms of the initial state of the coupled spin system, is then used to calculate the time-dependent muon-spin polarization. Finally this result is averaged over the initial (unpolarized) state of the electron spin and, when appropriate, over the rf phase.

Similar results could be obtained in other closely related ways, in particular by using density-matrix techniques[9] or by considering precession in an abstract vector space.[10] Our results are similar to those obtained for coherence effects in other types of experiments (see Sec. IV D). The differences arise primarily because of the high initial polarization of the muon and the direct observation of the time evolution of the muon-spin polarization that are characteristics of μSR.

This paper begins with a general derivation of the coupled differential equations which describe DEMUR for an arbitrary muoniumlike center (a coupled electron spin and muon spin with interactions appropriate for arbitrary symmetry). A general solution is then obtained for the case when the rf field is near resonance with just one transition with the neglect of all terms in the differential equations except the resultant near-secular terms. This general solution is then applied to muonium (isotropic hyperfine and Zeeman interactions). Among the results will be the equations needed to describe qualitatively and semiquantitatively the quartz DEMUR experiments discussed in a companion paper.[5] The general solution is then applied to the problems of the DEMUR of anomalous muonium in silicon, germanium, or diamond.[11-13] After this, other solutions of the differential equations will be discussed, such as a more accurate treatment of muonium needed for the quartz analysis and the treatment of nuclear hyperfine structure. Our results will then be compared with other types of magnetic resonance experiments on μ^+ and muonium and with other studies of coherence effects.

II. GENERAL THEORY

A. Formulation

A muoniumlike center in a crystal consists of an electron with unpaired spin bound by a positive muon. If the hyperfine interactions of the electron spin with nuclear spins in the crystal can be ignored, then the spin Hamiltonian of a muoniumlike center consists of three terms. These terms are the Zeeman interaction for the electron spin and for the muon spin and the hyperfine coupling between the two spins. By introducing an electronic g tensor $\overleftrightarrow{g}$ and a hyperfine tensor $\overleftrightarrow{A}$, the spin Hamiltonian can be written for arbitrary symmetry as[14]

$$\mathscr{H}=\mu_B\vec{H}\cdot\overleftrightarrow{g}\cdot\vec{S}-g_\mu\mu_\mu\vec{H}\cdot\vec{I}+\vec{S}\cdot\overleftrightarrow{A}\cdot\vec{I}\ , \tag{1}$$

where $\vec{H}$ is the total magnetic field, μ_B is the Bohr magneton, and $\frac{1}{2}g_\mu\mu_\mu$ is the muon magnetic moment. Although g_μ could deviate from its vacuum value (approximately equal to 2) and hence be slightly anisotropic in a crystal, these effects are small and can be neglected as they usually are for the nuclear Zeeman interaction of other paramagnetic centers in crystals.

In DEMUR, the magnetic field consists of two parts, a static component and a linearly-polarized rf component,[15]

$$\vec{H}=\vec{H}_0+\vec{H}_1\cos(\omega t+\phi)\ .$$

The time at which a μ^+ stops and traps an electron is taken to be $t=0$ and ϕ is the phase of the rf field at that time. The phase may be random[4,5] or specified,[16] depending on the experiment. We will assume that the muon is 100% polarized along the beam direction at $t=0$ and that the electron is completely unpolarized at that time.

The spin Hamiltonian of Eq. (1) can be separated into a time-independent part and a time-dependent part,

$$\mathcal{H}=\mathcal{H}_0+\mathcal{H}_1(t) ,$$

where

$$\mathcal{H}_0=\mu_B\vec{H}_0\cdot\overleftrightarrow{g}\cdot\vec{S}-g_\mu\mu_\mu\vec{H}_0\cdot\vec{I}+\vec{S}\cdot\overleftrightarrow{A}\cdot\vec{I} \tag{2}$$

and

$$\mathcal{H}_1(t)=(\mu_B\vec{H}_1\cdot\overleftrightarrow{g}\cdot\vec{S}-g_\mu\mu_\mu\vec{H}_1\cdot\vec{I})\cos(\omega t+\phi) .$$

There are four stationary states resulting from the solution of the eigenvalue problem using the time-independent Hamiltonian of Eq. (2). The stationary-state wave functions will be denoted by ψ_n and the energies by $\hbar\omega_n$. In terms of these stationary states a general time-dependent wave function may be written

$$\Psi(t)=\sum_{n=1}^{4} a_n(t)\psi_n e^{-i\omega_n t} , \tag{3}$$

where the $a_n(t)$ are time-dependent expansion coefficients. The initial values of the $a_n(t)$ are obtained in terms of the initial state of the system,

$$a_n(0)=\langle\psi_n\,|\,\Psi(0)\rangle , \tag{4}$$

where $\Psi(0)$ is the wave function of the system at $t=0$.[17] Substituting Eq. (3) for $\psi(t)$ into the full time-dependent Schrödinger equation we obtain four coupled differential equations for the $a_n(t)$:

$$\frac{da_m}{dt}=-i\sum_{n=1}^{4} a_n(t)\Omega_{mn}e^{i\omega_{mn}t}\cos(\omega t+\phi) , \tag{5}$$

where $\omega_{mn}\equiv\omega_m-\omega_n$ and

$$\hbar\Omega_{mn}\equiv\langle\psi_m\,|\,(\mu_B\vec{H}_1\cdot\overleftrightarrow{g}\cdot\vec{S}-g_\mu\mu_\mu\vec{H}_1\cdot\vec{I})\,|\,\psi_n\rangle .$$

Implicit in this approach is that there is no appreciable relaxation.

The observable quantity in any μSR experiment is the time-dependent polarization of the muon spin. In terms of the $a_n(t)$ this can be written as

$$\begin{aligned}\vec{P}(t)&=2\langle\Psi(t)\,|\,\vec{I}\,|\,\Psi(t)\rangle\\&=2\sum_{m,n=1}^{4} a_m^*(t)a_n(t)e^{i\omega_{mn}t}\langle\psi_m\,|\,\vec{I}\,|\,\psi_n\rangle .\end{aligned}$$

It is often convenient to write $\vec{P}(t)$ in terms of partial polarizations near the various transition frequencies ω_{mn} as

$$\vec{P}(t)=\vec{P}_0(t)+\sum_{m>n=1}^{4}\vec{P}_{mn}(t) , \tag{6}$$

where the partial polarization near zero frequency is

$$\vec{P}_0(t)=2\sum_{n=1}^{4}|a_n(t)|^2\langle\psi_n\,|\,\vec{I}\,|\,\psi_n\rangle \tag{7}$$

and

$$\vec{P}_{mn}(t)=4\,\mathrm{Re}[a_m^*(t)a_n(t)e^{i\omega_{mn}t}\langle\psi_m\,|\,\vec{I}\,|\,\psi_n\rangle] \tag{8}$$

is the partial polarization near the frequency ω_{mn}.

In summary the procedure to be followed is to first calculate the stationary states of the time-independent Hamiltonian of Eq. (2). These stationary states are then used to calculate the $a_n(0)$ in Eq. (4) and the coupled differential equations of Eq. (5). The differential equations are then solved in terms of the $a_n(0)$ from which $\vec{P}(t)$ is calculated using Eqs. (6), (7), and (8).

B. Solution for a muoniumlike center with a single driven transition

The coupled differential equations of Eq. (5) can be written as

$$\frac{da_m}{dt}=-\frac{i}{2}\sum_{n=1}^{4} a_n(t)\Omega_{mn}(e^{i(\omega+\omega_{mn})t}e^{i\phi}+e^{-i(\omega-\omega_{mn})t}e^{-i\phi}) . \tag{9}$$

If the specific frequency ω_{mn} ($\omega_{mn}>0$) is well separated from the other transition frequencies, then the rf frequency may be chosen to be near ω_{mn} and well separated from all other resonance frequencies. More precisely this condition is that

$$\begin{aligned}&|\omega-\omega_{mn}|\lesssim|\Omega_{mn}| ,\\&|\omega+\omega_{mn}|\gg|\Omega_{mn}| ,\\&|\omega\pm\omega_{ij}|\gg\Omega_{ij}|\quad(ij\neq mn) .\end{aligned}$$

Then the only terms on the right side of Eqs. (9) which we need to retain are those proportional to $\exp[\pm i(\omega-\omega_{mn})t]$, which then become

$$\begin{aligned}&\frac{da_k}{dt}=\frac{da_l}{dt}=0 ,\\&\frac{da_m}{dt}=-\frac{i}{2}\Omega_{mn}a_n(t)e^{-i(\omega-\omega_{mn})t}e^{-i\phi} ,\\&\frac{da_n}{dt}=-\frac{i}{2}\Omega_{mn}^*a_m(t)e^{i(\omega-\omega_{mn})t}e^{i\phi} ,\end{aligned} \tag{10}$$

where we have labeled the stationary states by the indices k, l, m, and n. The contributions of the neglected term to the $a_n(t)$ are of the order

$|\Omega_{ij}|/|\omega\pm\omega_{ij}|$

times that for the near secular term which we retain and thus small.

These equations can be solved by writing both $a_m(t)$ and $a_n(t)$ as Fourier series;

$$a_m(t)=\sum_i C_m^{(i)} e^{i\omega_m^{(i)}t} e^{-i\phi} ,$$
$$a_n(t)=\sum_i C_n^{(i)} e^{i\omega_n^{(i)}t} . \tag{11}$$

The values of $\omega_m^{(i)}$ and $\omega_n^{(i)}$ are related by

$$\omega_m^{(i)}=\omega_n^{(i)}-(\omega-\omega_{mn}) . \tag{12}$$

Substituting Eqs. (11) into Eqs. (10) and using Eq. (12) we obtain

$$(\omega_n^{(i)}-\omega+\omega_{mn})C_m^{(i)}+\tfrac{1}{2}\Omega_{mn}C_n^{(i)}=0 ,$$
$$\tfrac{1}{2}\Omega_{mn}^* C_m^{(i)}+\omega_n^{(i)}C_n^{(i)}=0 . \tag{13}$$

The equation for $\omega_n^{(i)}$ then becomes

$$\begin{vmatrix} \omega_n^{(i)}-\omega+\omega_{mn} & \tfrac{1}{2}\Omega_{mn} \\ \tfrac{1}{2}\Omega_{mn}^* & \omega_n^{(i)} \end{vmatrix} =0 ,$$

which yields

$$\omega_n^{(\pm)}=\tfrac{1}{2}[z\pm(z^2+1)^{1/2}]\,|\Omega_{mn}| \tag{14}$$

and

$$\omega_m^{(\pm)}=\tfrac{1}{2}[-z\pm(z^2+1)^{1/2}]\,|\Omega_{mn}| , \tag{15}$$

where we have denoted the two values by the superscripts $\pm$ and defined a reduced frequency displacement

$$z\equiv(\omega-\omega_{mn})/|\Omega_{mn}| . \tag{16}$$

Note that $\omega_n^{(\pm)}=-\omega_m^{(\mp)}$. Either of Eqs. (13) may then be used to relate $C_m^{(i)}$ to $C_n^{(i)}$. The values of $C_m^{(i)}$ or $C_n^{(i)}$ are then obtained from the initial values of $a_m(t)$ and $a_n(t)$. Calculating $a_m(t)$ and $a_n(t)$ in this way we obtain

$$a_m(t)=\frac{1}{2}\left[a_m(0)\left[1+\frac{z}{(z^2+1)^{1/2}}\right]-a_n(0)e^{-i(\phi-\phi_{mn})}\frac{1}{(z^2+1)^{1/2}}\right]e^{i\omega_m^{(+)}t}$$
$$+\frac{1}{2}\left[a_m(0)\left[1-\frac{z}{(z^2+1)^{1/2}}\right]+a_n(0)e^{-i(\phi-\phi_{mn})}\frac{1}{(z^2+1)^{1/2}}\right]e^{i\omega_m^{(-)}t} ,$$

$$a_n(t)=\frac{1}{2}\left[-a_m(0)e^{i(\phi-\phi_{mn})}\frac{1}{(z^2+1)^{1/2}}+a_n(0)\left[1-\frac{z}{(z^2+1)^{1/2}}\right]\right]e^{i\omega_n^{(+)}t}$$
$$+\frac{1}{2}\left[a_m(0)e^{i(\phi-\phi_{mn})}\frac{1}{(z^2+1)^{1/2}}+a_n(0)\left[1+\frac{z}{(z^2+1)^{1/2}}\right]\right]e^{i\omega_n^{(-)}t} ,$$

where ϕ_{mn} is defined by

$$e^{i\phi_{mn}}\equiv\Omega_{mn}/|\Omega_{mn}| .$$

In addition we have

$$a_k(t)=a_k(0) ,$$
$$a_l(t)=a_l(0) .$$

From these expressions for the $a_i(t)$, explicit expressions for $\vec{P}_0(t)$ and $\vec{P}_{ij}(t)$ can be obtained [see Eqs. (6)–(8)]. There are three types of terms $\vec{P}_{ij}(t)$ which are distinguishable by the relation between the indices i and j and the indices m and n labeling the driven transition.

If $ij=mn$ one obtains

$$\vec{P}_{mn}(t)=\mathrm{Re}\left[\langle\psi_m\mid\vec{I}\mid\psi_n\rangle\left\{\left[a_m^*(0)a_n(0)\left[1+\frac{z}{(z^2+1)^{1/2}}\right]^2\right.\right.$$
$$+[\,|a_m(0)|^2-|a_n(0)|^2]e^{i(\phi-\phi_{mn})}\frac{1}{(z^2+1)^{1/2}}\left[1+\frac{z}{(z^2+1)^{1/2}}\right]$$
$$\left.-a_m(0)a_n^*(0)e^{2i(\phi-\phi_{mn})}\frac{1}{z^2+1}\right]e^{i[\omega-(z^2+1)^{1/2}|\Omega_{mn}|]t}$$
$$+2\left[a_m^*(0)a_n(0)\frac{1}{z^2+1}-[\,|a_m(0)|^2-|a_n(0)|^2]e^{i(\phi-\phi_{mn})}\frac{z}{z^2+1}\right.$$
$$\left.+a_m(0)a_n^*(0)e^{2i(\phi-\phi_{mn})}\frac{1}{z^2+1}\right]e^{i\omega t}$$
$$+\left[a_m^*(0)a_n(0)\left[1-\frac{z}{(z^2+1)^{1/2}}\right]^2\right.$$
$$-[\,|a_m(0)|^2-|a_n(0)|^2]e^{i(\phi-\phi_{mn})}\frac{1}{(z^2+1)^{1/2}}\left[1-\frac{z}{(z^2+1)^{1/2}}\right]$$
$$\left.\left.-a_m(0)a_n^*(0)e^{2i(\phi-\phi_{mn})}\frac{1}{z^2+1}\right]e^{i[\omega+(z^2+1)^{1/2}|\Omega_{mn}|]t}\right\}\Bigg]. \tag{17}$$

The transition driven by the rf field is split into three lines with a splitting equal to $(z^2+1)^{1/2}|\Omega_{mn}|$, the Rabi frequency, and the central line at the rf frequency. The amplitudes of the three lines depend upon the rf phase relative to ϕ_{mn}, the rf frequency through z, and the initial state of the system through $a_m(0)$ and $a_n(0)$. For $|z|\gg 1$, the rf frequency is far from resonance and $\vec{P}_{mn}(t)$ reduces to

$$\vec{P}_{mn}(t)=4\,\mathrm{Re}[\langle\psi_m\mid\vec{I}\mid\psi_n\rangle a_m^*(0)a_n(0)e^{i\omega_{mn}t}],$$

the result for no applied rf field. For experiments which allow ϕ to be random we average over ϕ and thus all terms with a ϕ dependence in Eq. (17) are averaged to zero. Exactly on resonance, $z=0$, the random-phase partial polarization consists of three lines with amplitudes in the ratio 1:2:1.

For the case of $\vec{P}_{ij}(t)$ with only one index i or j being one of the indices m or n, there are four possibilities with similar but not identical results. The state involved can be m, the higher energy one, or n, the lower one. For each of these the state k, which is not an end state of the driven transition, may be above or below the appropriate end state. Thus the possibilities are

$$\vec{P}_{mk}(t)=2\,\mathrm{Re}\left[\langle\psi_m\mid\vec{I}\mid\psi_k\rangle\left\{\left[a_m^*(0)a_k(0)\left[1+\frac{z}{(z^2+1)^{1/2}}\right]\right.\right.\right.$$
$$\left.-a_n^*(0)a_k(0)e^{i(\phi-\phi_{nm})}\frac{1}{(z^2+1)^{1/2}}\right]e^{i(\omega_{mk}-\omega_m^{(+)})t}$$
$$+\left[a_m^*(0)a_k(0)\left[1-\frac{z}{(z^2+1)^{1/2}}\right]\right.$$
$$\left.\left.\left.+a_n^*(0)a_k(0)\,e^{i(\phi-\phi_{mn})}\frac{1}{(z^2+1)^{1/2}}\right]e^{i(\omega_{mk}-\omega_m^{(-)})t}\right\}\right], \tag{18}$$

$$\vec{P}_{nk}(t)=2\,\mathrm{Re}\left[\langle\psi_n\mid\vec{I}\mid\psi_k\rangle\left\{\left[-a_m^*(0)a_k(0)e^{-i(\phi-\phi_{mn})}\frac{1}{(z^2+1)^{1/2}}+a_n^*(0)a_k(0)\left[1-\frac{z}{(z^2+1)^{1/2}}\right]\right]e^{i(\omega_{nk}-\omega_n^{(+)})t}+\left[a_m^*(0)a_k(0)e^{-i(\phi-\phi_{mn})}\frac{1}{(z^2+1)^{1/2}}+a_n^*(0)a_k(0)\left[1+\frac{z}{(z^2+1)^{1/2}}\right]\right]e^{i(\omega_{nk}-\omega_n^{(-)})t}\right\}\right],$$

where $\omega_n^{(\pm)}$ and $\omega_m^{(\pm)}$ are given in Eqs. (14) and (15). $\vec{P}_{km}(t)$ and $\vec{P}_{kn}(t)$ are obtained from these results by replacing ω_{mk} by $-\omega_{km}$ or ω_{nk} by $-\omega_{kn}$. A transition with a single state in common with the transition driven by the rf magnetic field is split into two lines with a splitting of $(z^2+1)^{1/2}\mid\Omega_{mn}\mid$, the same splitting or Rabi frequency as obtained for the three lines of the driven transition [see Eq. (17)]. One of the two lines is above the precessional frequency for no rf and one is below it. For $\mid z\mid\gg1$, i.e., well off resonance, the expression for $\vec{P}_{mk}(t)$ in Eq. (18) becomes

$$\vec{P}_{mk}(t)=4\,\mathrm{Re}[\langle\psi_m\mid\vec{I}\mid\psi_k\rangle a_m^*(0)a_k(0)e^{i\omega_{mk}t}],$$

the result for no applied rf. Similar results occur for the other transition with only one state in common with the driven transition.

For experiments in which the rf phase at $t=0$ is random all ϕ-dependent terms average to zero. Exactly on resonance, $z=0$, one then obtains two lines of equal amplitude.

In the case that $ij=kl$, i.e., neither state of the driven transition is involved, the partial polarization is

$$\vec{P}_{kl}(t)=4\,\mathrm{Re}[\langle\psi_k\mid\vec{I}\mid\psi_l\rangle a_k^*(0)a_l(0)e^{i\omega_{kl}t}],$$

the result for no applied rf field.

Finally the low-frequency component $\vec{P}_0(t)$ is given by

$$\vec{P}_0(t)=2\sum_{i=1}^{4}\langle\psi_i\mid\vec{I}\mid\psi_i\rangle\mid a_i(0)\mid^2+2(\langle\psi_m\mid\vec{I}\mid\psi_m\rangle-\langle\psi_n\mid\vec{I}\mid\psi_n\rangle)\left[-\left[\tfrac{1}{2}(\mid a_m(0)\mid^2-\mid a_n(0)\mid^2)\frac{1}{z^2+1}+\mathrm{Re}(a_m^*(0)a_n(0)e^{-i(\phi-\phi_{mn})})\frac{z}{z^2+1}\right][1-\cos(\sqrt{z^2+1}\mid\Omega_{mn}\mid t)]+\mathrm{Im}(a_m^*(0)a_n(0)e^{-i(\phi-\phi_{nm})})\frac{1}{(z^2+1)^{1/2}}\sin(\sqrt{z^2+1}\mid\Omega_{mn}\mid t)\right]. \tag{19}$$

This consists of a static polarization, present even with no rf, plus a term which is significant only near resonance. The latter term consists of a static contribution whose amplitude depends on the rf frequency (or z) and an oscillation at a frequency equal to the frequency splittings or Rabi frequency obtained earlier [Eqs. (17) and (18)]. For a random rf phase the terms depending on ϕ are zero, a result which has a maximum oscillatory component exactly on resonance.

These results are valid for a case in which the rf is near resonance with one and only one transition, otherwise they apply quite generally to any muoniumlike center in solids so long as nuclear hyperfine structure can be ignored and there is negligible relaxation. In Sec. III A we particularize these results to muonium and in Sec. III B we will discuss the application to anomalous muonium or Mu* in Si, Ge, and diamond. To particularize these results to any muoniumlike center it is necessary to solve the time-dependent Schrödinger equation for the stationary states and then to calculate Ω_{mn}, the $a_i(0)$, and the $\langle\psi_i\mid\vec{I}\mid\psi_j\rangle$. It is also necessary to average over the random orientation of the electron spin which will appear in the expressions for $a_i(0)$ in all cases.

III. SPECIFIC RESULTS

A. Muonium with a single driven transition

The spin Hamiltonian for muonium has isotropic Zeeman and hyperfine interactions, thus Eq. (2) becomes

$$\mathcal{H}_0=g\mu_B\vec{H}_0\cdot\vec{S}-g_\mu\mu_\mu\vec{H}_0\cdot\vec{I}+A\vec{S}\cdot\vec{I}\ . \tag{20}$$

Although a very small anisotropy in $\overleftrightarrow{A}$ has been observed in crystalline quartz,[6,18] by incorporating a field-dependent effective[6] A, the results obtained from this isotropic spin Hamiltonian can be applied to the DEMUR of muonium in crystalline quartz.[4,5]

The solution of the eigenvalue problem represented by the Hamiltonian of Eq. (20) is well known.[2] Using as the basis $|M_S,M_I\rangle$, a product function of electron spin eigenfunctions $|M_S\rangle$, and muon spin functions $|M_I\rangle$, with the z axis chosen as the direction of $\vec{H}_0$, we can write the four muonium eigenfunctions as[19]

$$\begin{aligned}
\psi_1&=c\,|-\tfrac{1}{2},\tfrac{1}{2}\rangle-s\,|\tfrac{1}{2},-\tfrac{1}{2}\rangle\ ,\\
\psi_2&=|-\tfrac{1}{2},-\tfrac{1}{2}\rangle\ ,\\
\psi_3&=c\,|\tfrac{1}{2},-\tfrac{1}{2}\rangle+s\,|-\tfrac{1}{2},\tfrac{1}{2}\rangle\ ,\\
\psi_4&=|\tfrac{1}{2},\tfrac{1}{2}\rangle\ ,
\end{aligned} \tag{21}$$

where

$$\left.\begin{matrix}c\\ s\end{matrix}\right\}=\frac{1}{\sqrt{2}}\left[1\pm\frac{x}{(x^2+1)^{1/2}}\right]^{1/2} \tag{22}$$

and

$$x=\frac{g\mu_BH_0+g_\mu\mu_\mu H_0}{A}\ . \tag{23}$$

We will choose the x axis in order that $\vec{H}_1$ be in the z-x plane at an angle θ_1 with the z axis or $\vec{H}_0$. This completely determines the coordinate system, which is shown in Fig. 1. The direction of the beam, or more precisely the initial muon spin polarization $\vec{P}(0)$, is given by spherical polar angles θ_B and ϕ_B. The initial orientation of the muon spin is along $\vec{P}(0)$ but the initial orientation of the electron spin is random. We may describe the random initial orientations of the electron spin by specifying the spherical polar angles θ_e and ϕ_e and then, after calculation of $\vec{P}(t)$, the results are averaged over all possible orientations of the initial electron spin. It is convenient to write the wave function of muonium at $t=0$ as

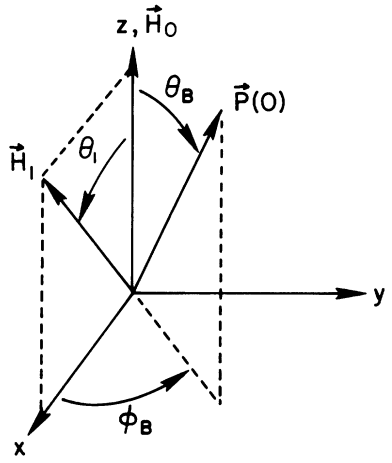

FIG. 1. Coordinate system used in describing DEMUR for muonium. The static field is along the z axis and the rf field is in the x-z plane.

$$\begin{aligned}
\Psi(0)=&\frac{\alpha}{\sqrt{2}}\sqrt{1+\cos\theta_B}\,|\tfrac{1}{2},\tfrac{1}{2}\rangle\\
&+\frac{\alpha}{\sqrt{2}}\sqrt{1-\cos\theta_B}\,e^{i\phi_B}\,|\tfrac{1}{2},-\tfrac{1}{2}\rangle\\
&+\frac{\beta}{\sqrt{2}}\sqrt{1+\cos\theta_B}\,|-\tfrac{1}{2},\tfrac{1}{2}\rangle\\
&+\frac{\beta}{\sqrt{2}}\sqrt{1-\cos\theta_B}\,e^{i\phi_B}\,|-\tfrac{1}{2},-\tfrac{1}{2}\rangle\ ,
\end{aligned} \tag{24}$$

where

$$\begin{aligned}
\alpha&=\frac{1}{\sqrt{2}}\sqrt{1+\cos\theta_e}\ ,\\
\beta&=\frac{1}{\sqrt{2}}\sqrt{1-\cos\theta_e}\,e^{i\phi_e}\ .
\end{aligned} \tag{25}$$

Upon averaging $\vec{P}(t)$ over θ_e and ϕ_e we find only four quantities appearing in the averages. The averages of these four quantities are

$$\begin{aligned}
&\langle\alpha^*\beta\rangle=\langle\alpha\beta^*\rangle=0\ ,\\
&\langle\,|\alpha|^2\rangle=\langle\,|\beta|^2\rangle=\tfrac{1}{2}\ .
\end{aligned} \tag{26}$$

In terms of α, β, θ_B, and ϕ_B, the values of $a_i(0)$ obtained using Eqs. (4) and (24) are

$$
\begin{aligned}
a_1(0)&=-\frac{\alpha s}{\sqrt{2}}\sqrt{1-\cos\theta_B}\,e^{i\phi_B}\\
&\quad+\frac{\beta c}{\sqrt{2}}\sqrt{1+\cos\theta_B}\ ,\\
a_2(0)&=\frac{\beta}{\sqrt{2}}\sqrt{1-\cos\theta_B}\,e^{i\phi_B}\ ,\\
a_3(0)&=\frac{\alpha c}{\sqrt{2}}\sqrt{1-\cos\theta_B}\,e^{i\phi_B}\\
&\quad+\frac{\beta s}{\sqrt{2}}\sqrt{1+\cos\theta_B}\ ,\\
a_4(0)&=\frac{\alpha}{\sqrt{2}}\sqrt{1+\cos\theta_B}\ .
\end{aligned}
\tag{27}
$$

It will prove useful to examine the results when each of three different transitions are driven by the rf magnetic field. These are the 4-3 and 3-2 transitions within the $F=1$ triplet, the transitions studied in the experiments on quartz,[4,5] and the 3-2 and 4-1 transitions which are the allowed electronic magnetic dipole transitions at high field. Thus we need to calculate three values of Ω_{ij}:

$$
\begin{aligned}
\hbar\Omega_{43}&=\tfrac{1}{2}\sin\theta_1(sg\mu_B H_1-cg_\mu\mu_\mu H_1)\ ,\\
\hbar\Omega_{32}&=\tfrac{1}{2}\sin\theta_1(cg\mu_B H_1-sg_\mu\mu_\mu H_1)\ ,\\
\hbar\Omega_{41}&=\tfrac{1}{2}\sin\theta_1(cg\mu_B H_1+sg_\mu\mu_\mu H_1)\ .
\end{aligned}
\tag{28}
$$

First consider the results for the rf frequency near resonance with the 4-3 transition. Since this case is primarily of interest for muonium at low fields we will ignore all contributions to $\vec{P}(t)$ involving state 1, the lowest state, because such high-frequency transitions are normally not observed. The remaining contributions to $\vec{P}(t)$ are obtained by substituting into Eqs. (17)–(19) with $\omega\simeq\omega_{43}$ and averaging over the orientation of the electron spin, using Eqs. (26) [also certain matrix elements of $\vec{I}$ must be calculated using Eqs. (21)]:

$$
\begin{aligned}
&\vec{P}_{42}(t)=0\ ,\\
&\vec{P}_{32}(t)=\tfrac{1}{4}s^2\sin\theta_B\left[\left[1-\frac{z}{(z^2+1)^{1/2}}\right]\{\hat{i}\cos[(\omega_{32}-\omega_+)t+\phi_B]+\hat{j}\sin[(\omega_{32}-\omega_+)t+\phi_B]\}\right.\\
&\qquad\left.+\left[1+\frac{z}{(z^2+1)^{1/2}}\right]\{\hat{i}\cos[(\omega_{32}+\omega_-)t+\phi_B]+\hat{j}\sin[(\omega_{32}+\omega_-)t+\phi_B]\}\right]\ ,\\
&\vec{P}_{43}(t)=\tfrac{1}{8}c^2\mathrm{Re}\left[(\hat{i}-i\hat{j})\left\{\left[\left[1+\frac{z}{(z^2+1)^{1/2}}\right]^2\sin\theta_B+\frac{1}{(z^2+1)^{1/2}}\left[1+\frac{z}{(z^2+1)^{1/2}}\right]2c\cos\theta_B e^{i(\phi-\phi_B)}\right.\right.\right.\\
&\qquad\left.-\frac{1}{z^2+1}\sin\theta_B\,e^{2i(\phi-\phi_B)}\right]\exp[i(\omega-\sqrt{z^2+1}\,\Omega_{43})t+i\phi_B]\\
&\qquad+2\left[\frac{1}{z^2+1}\sin\theta_B-\frac{z}{z^2+1}2c\cos\theta_B e^{i(\phi-\phi_B)}+\frac{1}{z^2+1}\sin\theta_B e^{2i(\phi-\phi_B)}\right]\exp[i(\omega t+\phi_B)]\\
&\qquad+\left[\left[1-\frac{z}{(z^2+1)^{1/2}}\right]^2\sin\theta_B-\frac{1}{(z^2+1)^{1/2}}\left[1-\frac{z}{(z^2+1)^{1/2}}\right]2c\cos\theta_B e^{i(\phi-\phi_B)}\right.\\
&\qquad\left.\left.\left.-\frac{1}{z^2+1}\sin\theta_B\,e^{2i(\phi-\phi_B)}\right]\exp[i(\omega+\sqrt{z^2+1}\,\Omega_{43})t+i\phi_B]\right\}\right]\ ,\\
&\vec{P}_0(t)=\hat{k}\left[(1-2s^2c^2)\cos\theta_B-\tfrac{1}{2}c^3\left[c\frac{1}{z^2+1}\cos\theta_B+\frac{z}{z^2+1}\sin\theta_B\cos(\phi-\phi_B)\right]\right.\\
&\qquad\left.\times(1-\cos\sqrt{z^2+1}\,\Omega_{43}t)-\tfrac{1}{2}c^3\frac{1}{(z^2+1)^{1/2}}\sin\theta_B\sin(\phi-\phi_B)\sin(\sqrt{z^2+1}\,\Omega_{43}t)\right]\ ,
\end{aligned}
\tag{29}
$$

where

$$z=(\omega-\omega_{43})/\Omega_{43}\ ,$$

$$\omega_\pm=\tfrac{1}{2}[(z^2+1)^{1/2}\pm z]\Omega_{43}\ ,$$

and Ω_{43} is evaluated in Eqs. (28). The unit vectors in the x, y, and z directions are $\hat{i}$, $\hat{j}$, and $\hat{k}$, respectively. There is no dependence of $\vec{P}_{32}(t)$ on the rf phase but $\vec{P}_0(t)$ and especially $\vec{P}_{43}(t)$ are quite complicated for a fixed rf phase. For random phase these two terms simplify to

$$\begin{aligned}\vec{P}_{43}(t)=&\tfrac{1}{8}c^2\sin\theta_B\left[\left[1+\frac{z}{(z^2+1)^{1/2}}\right]^2\{\hat{i}\cos[(\omega-\sqrt{z^2+1}\Omega_{43})t+\phi_B]\right.\\&\left.+\hat{j}\sin[(\omega-\sqrt{z^2+1}\Omega_{43})t+\phi_B]\}\right.\\&+\frac{2}{z^2+1}[\hat{i}\cos(\omega t+\phi_B)+\hat{j}\sin(\omega t+\phi_B)]\\&+\left[1-\frac{z}{(z^2+1)^{1/2}}\right]^2\{\hat{i}\cos[(\omega+\sqrt{z^2+1}\Omega_{43})t+\phi_B]\\&\left.+\hat{j}\sin[(\omega+\sqrt{z^2+1}\Omega_{43})t+\phi_B]\}\right],\\\vec{P}_0(t)=&\hat{k}\cos\theta_B\left[1-2s^2c^2-\tfrac{1}{2}c^4\frac{1}{z^2+1}[1-\cos(\sqrt{z^2+1}\Omega_{43}t)]\right].\end{aligned}\tag{30}$$

The second case of interest is when ω is nearly resonant with ω_{32}. In the low static-field region this case is examined experimentally in a companion paper for muonium in quartz.[4,5] In the high-field region this case is an example of DEMUR in which the driven EPR transition is not observable in μSR. This could occur for isotropic muoniumlike entities with small hyperfine splittings, such as are observed for muonic free radicals in liquids.[20] To understand both limits all components of $\vec{P}(t)$ are calculated. As before $\vec{P}_{42}(t)$ is zero and $\vec{P}_{41}(t)$ is unaffected by the rf field. Thus for $\omega\simeq\omega_{32}$,

$$\begin{aligned}\vec{P}_{43}(t)=&\tfrac{1}{4}c^2\sin\theta_B\left[\left[1-\frac{z}{(z^2+1)^{1/2}}\right]\{\hat{i}\cos[(\omega_{43}-\omega_+)t+\phi_B]+\hat{j}\sin[(\omega_{43}-\omega_+)t+\phi_B]\}\right.\\&\left.+\left[1+\frac{z}{(z^2+1)^{1/2}}\right]\{\hat{i}\cos[(\omega_{43}+\omega_-)t+\phi_B]+\hat{j}\sin[(\omega_{43}+\omega_-)t+\phi_B]\}\right],\\\vec{P}_{21}(t)=&\tfrac{1}{4}c^2\mathrm{Re}\left[(\hat{i}+i\hat{j})\left\{\left[\left[1-\frac{z}{(z^2+1)^{1/2}}\right]\sin\theta_B\right.\right.\right.\\&\left.\left.\left.-\frac{1}{(z^2+1)^{1/2}}2s\cos\theta_B e^{-i(\phi-\phi_B)}\right]\exp[i(\omega_{21}-\omega_+)t-i\phi_B]\right.\\&+\left[\left[1+\frac{z}{(z^2+1)^{1/2}}\right]\sin\theta_B+\frac{1}{(z^2+1)^{1/2}}2s\cos\theta_B e^{-i(\phi-\phi_B)}\right]\\&\left.\left.\times\exp[i(\omega_{21}+\omega_-)t-i\phi_B]\right\}\right],\\\vec{P}_{31}(t)=&sc^2\hat{k}\,\mathrm{Re}\left\{\left[\left[1+\frac{z}{(z^2+1)^{1/2}}\right]s\cos\theta_B-\frac{1}{2}\frac{1}{(z^2+1)^{1/2}}\sin\theta_B e^{i(\phi-\phi_B)}\right]\exp[i(\omega_{31}-\omega_-)t]\right.\\&\left.+\left[\left[1-\frac{z}{(z^2+1)^{1/2}}\right]s\cos\theta_B+\frac{1}{2}\frac{1}{(z^2+1)^{1/2}}\sin\theta_B e^{i(\phi-\phi_B)}\right]\exp[i(\omega_{31}+\omega_+)t]\right\},\end{aligned}\tag{31}$$

$$\vec{P}_{32}(t)=\tfrac{1}{8}s^2\mathrm{Re}\left[(\hat{i}-i\hat{j})\left\{\left[\left[1+\frac{z}{(z^2+1)^{1/2}}\right]^2\sin\theta_B+\frac{1}{(z^2+1)^{1/2}}\left[1+\frac{z}{(z^2+1)^{1/2}}\right]2s\cos\theta_B e^{i(\phi-\phi_B)}\right.\right.$$
$$\left.-\frac{1}{z^2+1}\sin\theta_B e^{2i(\phi-\phi_B)}\right]\exp[i(\omega-\sqrt{z^2+1}\,\Omega_{32})t+i\phi_B]$$
$$+2\left[\frac{1}{z^2+1}\sin\theta_B-\frac{z}{z^2+1}2s\cos\theta_B e^{i(\phi-\phi_B)}\right.$$
$$\left.+\frac{1}{z^2+1}\sin\theta_B e^{2i(\phi-\phi_B)}\right]\exp[i(\omega t+\phi_B)]$$
$$+\left[\left[1-\frac{z}{(z^2+1)^{1/2}}\right]^2\sin\theta_B-\frac{1}{(z^2+1)^{1/2}}\left[1-\frac{z}{(z^2+1)^{1/2}}\right]2s\cos\theta_B e^{i(\phi-\phi_B)}\right.$$
$$\left.\left.-\frac{1}{z^2+1}\sin\theta_B e^{2i(\phi-\phi_B)}\right]\exp[i(\omega+\sqrt{z^2+1}\,\Omega_{32})t+i\phi_B]\right\}\Bigg],$$

$$\vec{P}_0(t)=\hat{k}\left[(1-2s^2c^2)\cos\theta_B-\tfrac{1}{2}s^3\left[s\frac{1}{z^2+1}\cos\theta_B+\frac{z}{z^2+1}\sin\theta_B\cos(\phi-\phi_B)\right]\right.$$
$$\left.\times[1-\cos(\sqrt{z^2+1}\,\Omega_{32}t)]-\tfrac{1}{2}s^3\frac{1}{(z^2+1)^{1/2}}\sin\theta_B\sin(\phi-\phi_B)\sin(\sqrt{z^2+1}\,\Omega_{32}t)\right],$$

where

$$z=(\omega-\omega_{32})/\Omega_{32},$$
$$\omega_\pm=\tfrac{1}{2}(\sqrt{z^2+1}\pm z)\Omega_{32},$$

and Ω_{32} is given in Eqs. (28). For random rf phase ϕ, $\vec{P}_{21}(t)$ becomes identical to $\vec{P}_{43}(t)$ except that the arguments of sine and cosine are $(\omega_{21}\mp\omega_\pm)t-\phi_B$ and the sign of $\hat{j}$ is changed, i.e., the sense of precession of the μ^+ spin is reversed, a result found for zero rf field. For random ϕ, $\vec{P}_{32}(t)$ and $\vec{P}_0(t)$ are identical to $\vec{P}_{43}(t)$ and $\vec{P}_0(t)$ in Eqs. (30) except that s and c must be interchanged and Ω_{43} replaced by Ω_{32}. For random ϕ, $\vec{P}_{31}(t)$ becomes

$$\vec{P}_{31}(t)=s^2c^2\cos\theta_B\hat{k}\left[\left[1+\frac{z}{(z^2+1)^{1/2}}\right]\cos[(\omega_{31}-\omega_-)t]+\left[1-\frac{z}{(z^2+1)^{1/2}}\right]\cos[(\omega_{31}+\omega_+)t]\right].$$

For the final case, ω near resonance with the transition at ω_{41}, $\vec{P}_{42}(t)$ is again zero and $\vec{P}_{32}(t)$ is unaffected by the rf field. Thus for $\omega\simeq\omega_{41}$ we have

$$\vec{P}_{43}(t)=\tfrac{1}{4}c^2\mathrm{Re}\left[(\hat{i}-i\hat{j})\left\{\left[\left[1+\frac{z}{(z^2+1)^{1/2}}\right]\sin\theta_B-\frac{1}{(z^2+1)^{1/2}}2s\cos\theta_B e^{i(\phi-\phi_B)}\right]\right.\right.$$
$$\times\exp[i(\omega_{43}-\omega_-)t+i\phi_B]$$
$$+\left[\left[1-\frac{z}{(z^2+1)^{1/2}}\right]\sin\theta_B+\frac{1}{(z^2+1)^{1/2}}2s\cos\theta_B e^{i(\phi-\phi_B)}\right]$$
$$\left.\left.\times\exp[i(\omega_{43}+\omega_+)t+i\phi_B]\right\}\right],$$

$$\vec{P}_{21}(t)=\tfrac{1}{4}c^2\sin\theta_B\left[\left[1+\frac{z}{(z^2+1)^{1/2}}\right]\{\hat{i}\cos[(\omega_{21}-\omega_-)t-\phi_B]-\hat{j}\sin[(\omega_{21}-\omega_-)t-\phi_B]\}\right.$$

$$\left.+\left[1-\frac{z}{(z^2+1)^{1/2}}\right]\{\hat{i}\cos[(\omega_{21}+\omega_+)t-\phi_B]-\hat{j}\sin[(\omega_{21}+\omega_+)t-\phi_B]\}\right],$$

$$\vec{P}_{31}(t)=sc^2\hat{k}\,\mathrm{Re}\left\{\left[\left[1+\frac{z}{(z^2+1)^{1/2}}\right]s\cos\theta_B+\frac{1}{2}\frac{1}{(z^2+1)^{1/2}}\sin\theta_B e^{i(\phi-\phi_B)}\right]\exp[i(\omega_{31}-\omega_-)t]\right.$$

$$\left.+\left[\left[1-\frac{z}{(z^2+1)^{1/2}}\right]s\cos\theta_B-\frac{1}{2}\frac{1}{(z^2+1)^{1/2}}\sin\theta_B e^{i(\phi-\phi_B)}\right]\exp[i(\omega_{31}+\omega_+)t]\right\},$$

$$\vec{P}_{41}(t)=\tfrac{1}{8}s^2\,\mathrm{Re}\left[(\hat{i}-i\hat{j})\left\{\left[\left[1+\frac{z}{(z^2+1)^{1/2}}\right]^2\sin\theta_B-\frac{1}{(z^2+1)^{1/2}}\left[1+\frac{z}{(z^2+1)^{1/2}}\right]2s\cos\theta_B e^{i(\phi-\phi_B)}\right.\right.\right. \tag{32}$$

$$\left.-\frac{1}{z^2+1}\sin\theta_B e^{2i(\phi-\phi_B)}\right]\exp[i(\omega-\sqrt{z^2+1}\,\Omega_{41})t+i\phi_B]$$

$$+2\left[\frac{1}{z^2+1}\sin\theta_B+\frac{z}{z^2+1}2s\cos\theta_B e^{i(\phi-\phi_B)}+\frac{1}{z^2+1}\sin\theta_B e^{2i(\phi-\phi_B)}\right]\exp[i(\omega t+\phi_B)]$$

$$+\left[\left[1-\frac{z}{(z^2+1)^{1/2}}\right]^2\sin\theta_B+\frac{1}{(z^2+1)^{1/2}}\left[1-\frac{z}{(z^2+1)^{1/2}}\right]2s\cos\theta_B e^{i(\phi-\phi_B)}\right.$$

$$\left.\left.\left.-\frac{1}{z^2+1}\sin\theta_B\ e^{2i(\phi-\phi_B)}\right]\exp[i(\omega+\sqrt{z^2+1}\,\Omega_{41})t+i\phi_B]\right\}\right],$$

$$\vec{P}_0(t)=\hat{k}\left[(1-2s^2c^2)\cos\theta_B-\tfrac{1}{2}s^3\left[s\frac{1}{z^2+1}\cos\theta_B-\frac{z}{z^2+1}\sin\theta_B\cos(\phi-\phi_B)\right]\right.$$

$$\left.\times[1-\cos(\sqrt{z^2+1}\,\Omega_{41}t)]+\tfrac{1}{2}s^3\frac{1}{(z^2+1)^{1/2}}\sin\theta_B\sin(\phi-\phi_B)\sin(\sqrt{z^2+1}\,\Omega_{41}t)\right],$$

where

$$z=(\omega-\omega_{41})/\Omega_{41},$$

$$\omega_\pm=\tfrac{1}{2}(\sqrt{z^2+1}\pm z)\Omega_{41},$$

and Ω_{41} is given in Eqs. (28). The results for random rf phase can be calculated as in previous cases.

B. Selected results for anomalous muonium with a single driven transition

A muoniumlike center with a small but very anisotropic hyperfine interaction has been observed in each of diamond, silicon, and germanium.[11–13] These centers have been designated anomalous muonium (or Mu*). Detailed μSR studies have shown that these centers have axial symmetry about one of the crystalline ⟨111⟩ axes. The spin Hamiltonian for anomalous muonium, including an axial electronic g tensor, is

$$\mathcal{H}_0=g_{\|}\mu_B H_z S_z+g_\perp\mu_B(H_xS_x+H_yS_y)$$

$$-g_\mu\mu_\mu\vec{H}\cdot\vec{I}+A_{\|}S_zI_z+A_\perp(S_xI_x+S_yI_y),$$

where the z direction is the $\langle 111 \rangle$ symmetry axis of the specific Mu* under study (there are four possible orientations, all of which are observed with equal probability).

Although the g and A tensors are much simpler in this case than the most complicated (lowest-symmetry) possibility allowed in the general analysis of Sec. II, there is very little simplification possible of those general results for an arbitrary orientation of the magnetic field. However, one reason for studying the DEMUR of Mu* is to measure the principal values of the g tensor. To do this it is most convenient to study Mu* centers whose symmetry axes are either parallel to the magnetic field (to measure $g_{||}$) or perpendicular to it (to measure $g_{\perp}$). In addition the greatest precision is obtained by measurements made at high field where the EPR transitions are so weak in the μSR that they would be difficult or impossible to observe. These conditions simplify the general results and limit the contributions to $\vec{P}(t)$ that are observable.

The spin Hamiltonian for the case of the static magnetic field parallel to the symmetry axis is

$$\mathcal{H}_0 = g_{||}\mu_B H_0 S_z - g_\mu \mu_\mu H_0 I_z + A_{||} S_z I_z + A_\perp (S_x I_x + S_y I_y) .$$

This Hamiltonian is somewhat similar to that of Eq. (20) when the field defines the z axis. This leads to eigenfunctions identical to those of Eq. (21) except that the variable x in Eq. (23) is given by

$$x = \frac{g_{||}\mu_B H_0 + g_\mu \mu_\mu H_0}{A_\perp} .$$

Defining the geometry as shown in Fig. 1, we obtain the initial values of the a_i given in Eq. (27) and the expressions for Ω_{ij} given in Eq. (28) with g replaced by $g_\perp$. The only other major difference between this case and that of muonium presented in Sec. III A is that either levels 3 and 4 or levels 1 and 2 cross for Mu*. We will continue to label the states as in Eq. (21). This is illustrated in Fig. 2 for the case of diamond.[13] For those regions of field in which the order is reversed it will be necessary to replace ω_{43} by $-\omega_{34}$ or ω_{21} by $-\omega_{12}$ in the equations of Sec. III A. The allowed electronic magnetic dipole transitions at high field are 3-2 and 4-1 as for muonium; thus we will be interested in only two cases. The first case is with the rf frequency close to ω_{32} only, where the results of Eqs. (31) for $\vec{P}_{43}(t)$ and $\vec{P}_{21}(t)$ give the important components of $\vec{P}(t)$. Similarly, if ω is near ω_{41} only, then $\vec{P}_{43}(t)$ and $\vec{P}_{21}(t)$ are obtained from Eqs. (32).

Results for the static magnetic field perpendicular to the Mu* symmetry axis are somewhat different. The static spin Hamiltonian for this orientation of

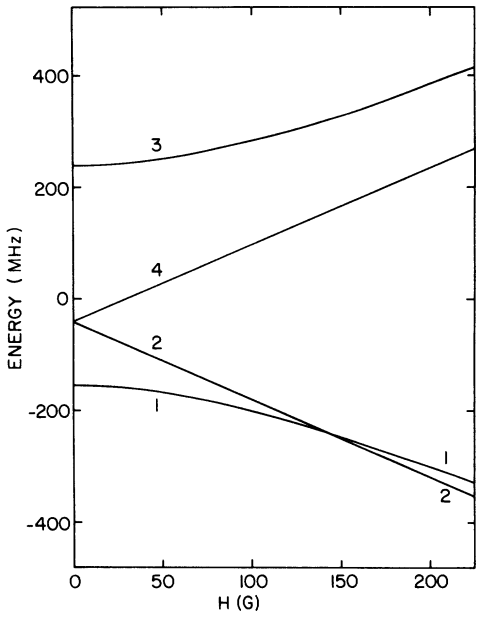

FIG. 2. Energy-level diagram for Mu* in diamond when the static field is parallel to the Mu* symmetry axis. The labeling of the states is shown. This is the same as that used for muonium if level 3 were degenerate with levels 2 and 4 at $H=0$.

the field can be written as

$$\mathcal{H}_0 = g_\perp \mu_B H_0 S_z - g_\mu \mu_\mu H_0 I_z + A_\perp S_z I_z + \tfrac{1}{4}(A_\perp + A_{||})(S_+ I_- + S_- I_+) + \tfrac{1}{4}(A_\perp - A_{||})(S_+ I_+ + S_- I_-) .$$

The eigenfunctions for this Hamiltonian are

$$\begin{aligned} \psi_1 &= c_+ \left| -\tfrac{1}{2}, \tfrac{1}{2} \right\rangle - s_+ \left| \tfrac{1}{2}, -\tfrac{1}{2} \right\rangle , \\ \psi_2 &= c_- \left| -\tfrac{1}{2}, -\tfrac{1}{2} \right\rangle - s_- \left| \tfrac{1}{2}, \tfrac{1}{2} \right\rangle , \\ \psi_3 &= c_+ \left| \tfrac{1}{2}, -\tfrac{1}{2} \right\rangle + s_+ \left| -\tfrac{1}{2}, \tfrac{1}{2} \right\rangle , \\ \psi_4 &= c_- \left| \tfrac{1}{2}, \tfrac{1}{2} \right\rangle + s_- \left| -\tfrac{1}{2}, -\tfrac{1}{2} \right\rangle , \end{aligned} \tag{33}$$

where $c_\pm$ and $s_\pm$ are given by Eq. (22) with the variables $x_\pm$ given by

$$x_\pm = \frac{g_\perp \mu_B H_0 + g_\mu \mu_\mu H_0}{\frac{1}{2}(A_\perp \pm A_{||})} .$$

For this case the states will be labeled from lowest to highest energy at low field. The 3 and 4 levels cross at fields which are too high for DEMUR experiments. The initial state of Mu* in terms of the

beam orientation and the electron variables of Eqs. (25) are identical to Eq. (24) as it was in the parallel case. However, since the eigenfunctions of Eq. (33) are different from the muonium functions of Eq. (21), the values of $a_i(0)$ will differ. They are

$$a_1(0)=\frac{\beta c_+}{\sqrt{2}}\sqrt{1+\cos\theta_B} - \frac{\alpha s_+}{\sqrt{2}}\sqrt{1-\cos\theta_B}e^{i\phi_B} ,$$

$$a_2(0)=\frac{\beta c_-}{\sqrt{2}}\sqrt{1-\cos\theta_B}e^{i\phi_B} - \frac{\alpha s_-}{\sqrt{2}}\sqrt{1+\cos\theta_B} ,$$

$$a_3(0)=\frac{\alpha c_+}{\sqrt{2}}\sqrt{1-\cos\theta_B}e^{i\phi_B} + \frac{\beta s_+}{\sqrt{2}}\sqrt{1+\cos\theta_B} ,$$

$$a_4(0)=\frac{\alpha c_-}{\sqrt{2}}\sqrt{1+\cos\theta_B} + \frac{\beta s_-}{\sqrt{2}}\sqrt{1-\cos\theta_B}e^{i\phi_B} ,$$

where α and β are given in Eqs. (25).

Calculation of the Ω_{ij} is more complicated here than in the earlier examples. The coordinate system and the various directions of importance are shown in Fig. 3. The expressions for the two Ω_{ij} of interest are

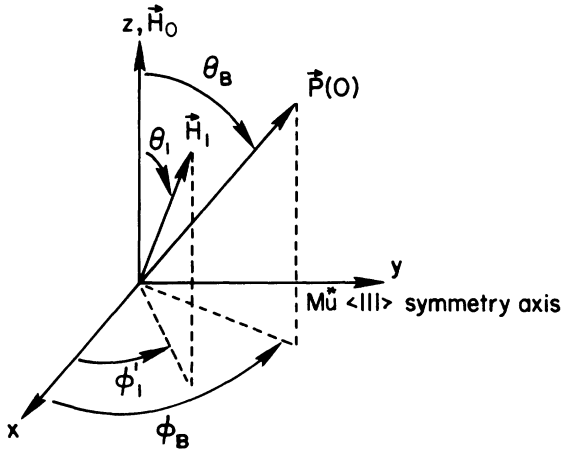

FIG. 3. Coordinate system used in describing DEMUR for Mu* when the static field is perpendicular to the Mu* symmetry axis. The static field is along the z axis, the Mu* symmetry axis is the y axis, and $\vec{H}_1$ and $\vec{P}(0)$ are specified by spherical polar angles.

$$\hbar\Omega_{32}=\tfrac{1}{2}\sin\theta_1[g\mu_B H_1(c_+c_-e^{-i\phi_1}-s_+s_-e^{i\phi_1})-g_\mu\mu_\mu H_1(c_-s_+e^{-i\phi_1}-c_+s_-e^{i\phi_1})] ,$$

$$\hbar\Omega_{41}=\tfrac{1}{2}\sin\theta_1[g\mu_B H_1(c_+c_-e^{-i\phi_1}-s_+s_-e^{i\phi_1})+g_\mu\mu_\mu H_1(c_-s_+e^{-i\phi_1}-c_+s_-e^{i\phi_1})] ,$$

where

$$g=(g_\perp^2\cos^2\phi_1'+g_{||}^2\sin^2\phi_1')^{1/2} ,$$

$$\phi_1=\tan^{-1}\left[\frac{g_{||}}{g_\perp}\tan\phi_1'\right] .$$

These are equivalent to the values in Eqs. (28) when $\phi_1=0$, $s_-=0$, and $c_-=1$, as expected. Note that the Ω_{ij} are not in general real, so that ϕ_{ij} will not necessarily be zero. The results for $\langle\psi_i\,|\,\vec{I}\,|\,\psi_j\rangle$ are more complicated; the required values are

$$\langle\psi_4\,|\,\vec{I}\,|\,\psi_3\rangle=\tfrac{1}{2}(c_+c_-+s_+s_-)\hat{i}-\frac{i}{2}(c_+c_--s_+s_-)\hat{j} ,$$

$$\langle\psi_2\,|\,\vec{I}\,|\,\psi_1\rangle=\tfrac{1}{2}(c_+c_-+s_+s_-)\hat{i}+\frac{i}{2}(c_+c_--s_+s_-)\hat{j} .$$

If the rf frequency is near ω_{32} only, then the principal components of $\vec{P}(t)$ (aside from a nearly constant static contribution if $\theta_B\neq\pi/2$) are

$$\vec{P}_{43}(t)=\tfrac{1}{4}\,\mathrm{Re}\Bigg[[(c_+c_-+s_+s_-)\hat{i}-i(c_+c_--s_+s_-)\hat{j}]$$
$$\times\Bigg\{\Bigg[\Bigg[1-\frac{z}{(z^2+1)^{1/2}}\Bigg]\sin\theta_B(c_+c_-e^{i\phi_B}+s_+s_-e^{-i\phi_B})$$
$$-\frac{1}{(z^2+1)^{1/2}}2s_-c_-\cos\theta_B e^{-i(\phi-\phi_{32})}\Bigg]\exp[i(\omega_{43}-\omega_+)t]$$
$$+\Bigg[\Bigg[1+\frac{z}{(z^2+1)^{1/2}}\Bigg]\sin\theta_B(c_+c_-e^{i\phi_B}+s_+s_-e^{-i\phi_B})$$
$$+\frac{1}{(z^2+1)^{1/2}}2s_-c_-\cos\theta_B e^{-i(\phi-\phi_{32})}\Bigg]\exp[i(\omega_{43}+\omega_-)t]\Bigg\}\Bigg],$$

$$\vec{P}_{21}(t)=\tfrac{1}{4}\,\mathrm{Re}\Bigg[[(c_+c_-+s_+s_-)\hat{i}+i(c_+c_--s_+s_-)\hat{j}]$$
$$\times\Bigg\{\Bigg[\Bigg[1-\frac{z}{(z^2+1)^{1/2}}\Bigg]\sin\theta_B(c_+c_-e^{-i\phi_B}+s_+s_-e^{i\phi_B})$$
$$-\frac{1}{(z^2+1)^{1/2}}2s_+c_+\cos\theta_B e^{-i(\phi-\phi_{32})}\Bigg]\exp[i(\omega_{21}-\omega_+)t]$$
$$+\Bigg[\Bigg[1+\frac{z}{(z^2+1)^{1/2}}\Bigg]\sin\theta_B(c_+c_-e^{-i\phi_B}+s_+s_-e^{i\phi_B})$$
$$+\frac{1}{(z^2+1)^{1/2}}2s_+c_+\cos\theta_B e^{-i(\phi-\phi_{32})}\Bigg]\exp[i(\omega_{21}+\omega_-)t]\Bigg\}\Bigg],$$

where

$$z=(\omega-\omega_{32})/|\Omega_{32}|\ ,$$

$$\omega_\pm=\tfrac{1}{2}(\sqrt{z^2+1}\pm z)\,|\Omega_{32}|\ .$$

We note here that the dependence of $\vec{P}_{43}(t)$ and $\vec{P}_{21}(t)$ upon the rf phase angle ϕ is only present if there is a component of the beam along the static field. Even then they are weak at high fields.

Rather similar results are obtained when ω is close to ω_{41} but not close to ω_{32}, i.e.,

$$\vec{P}_{43}(t)=\tfrac{1}{4}\,\mathrm{Re}\Bigg[[(c_+c_-+s_+s_-)\hat{i}-i(c_+c_--s_+s_-)\hat{j}]$$
$$\times\Bigg\{\Bigg[\Bigg[1+\frac{z}{(z^2+1)^{1/2}}\Bigg]\sin\theta_B(c_+c_-e^{i\phi_B}+s_+s_-e^{-i\phi_B})$$
$$-\frac{1}{(z^2+1)^{1/2}}2s_+c_+\cos\theta_B e^{i(\phi-\phi_{41})}\Bigg]\exp[i(\omega_{43}-\omega_-)t]$$
$$+\Bigg[\Bigg[1-\frac{z}{(z^2+1)^{1/2}}\Bigg]\sin\theta_B(c_+c_-e^{i\phi_B}+s_+s_-e^{-i\phi_B})$$
$$+\frac{1}{(z^2+1)^{1/2}}2s_+c_+\cos\theta_B\, e^{i(\phi-\phi_{41})}\Bigg]\exp[i(\omega_{43}+\omega_+)t]\Bigg\}\Bigg],$$

$$\vec{P}_{21}(t)=\tfrac{1}{4}\,\mathrm{Re}\Bigg\{[(c_+c_-+s_+s_-)\hat{i}+i(c_+c_--s_+s_-)\hat{j}]$$
$$\times\Bigg\{\Bigg[\Bigg[1+\frac{z}{(z^2+1)^{1/2}}\Bigg]\sin\theta_B(c_+c_-e^{-i\phi_B}+s_+s_-e^{i\phi_B})$$
$$-\frac{1}{(z^2+1)^{1/2}}2s_-c_-\cos\theta_B e^{i(\phi-\phi_{41})}\Bigg]\exp[i(\omega_{21}-\omega_-)t]$$
$$+\Bigg[\Bigg[1-\frac{z}{(z^2+1)^{1/2}}\Bigg]\sin\theta_B(c_+c_-e^{-i\phi_B}+s_+s_-e^{i\phi_B})$$
$$+\frac{1}{(z^2+1)^{1/2}}2s_-c_-\cos\theta_B e^{i(\phi-\phi_{41})}\Bigg]\exp[i(\omega_{21}+\omega_+)t]\Bigg\}\Bigg]\Bigg\},$$

where

$$z=(\omega-\omega_{41})/|\Omega_{41}|\ ,$$
$$\omega_\pm=\tfrac{1}{2}(\sqrt{z^2+1}\pm z)\,|\Omega_{41}|\ .$$

Thus for Mu* with the external field either parallel to or perpendicular to the symmetry axis, it is possible to determine the resonance frequencies of the EPR transitions by the requirement that the two DEMUR lines near ω_{43} or ω_{21} have equal amplitude if random rf phase is used, if the beam is perpendicular to the static magnetic field, or if the static magnetic field is large enough. To find this condition involves a search in which the rf frequency or the static magnetic field is varied. One must know in which sense to change the frequency and by approximately how much. The previous analysis gives this information but we here make it explicit.

If the two lines near ω_{43} and the two lines near ω_{21} both have the lower frequency line more intense, then ω is less than ω_{32} or greater than ω_{41}; it is not possible to tell from this which resonance is closer to the rf frequency. If the upper frequency lines are more intense, then ω is greater than ω_{32} or less than ω_{41}. This applies to the case when $\vec{H}$ is perpendicular to the symmetry axis and also to the case when they are parallel, provided that level 4 is above level 3 and level 2 is above level 1.

The next step is to calculate the ratio of the amplitudes of the strongest to the weakest line of any pair split by the application of the rf field (or preferably a suitable average of both pairs). Calling this ratio ρ we have

$$\rho=\frac{1+|z|(z^2+1)^{-1/2}}{1-|z|(z^2+1)^{-1/2}}\ .$$

From this, the measured splitting (or average of the splittings)

$$\Delta\omega=\sqrt{z^2+1}\,|\Omega_{mn}|\ ,$$

and the definition of z in Eq. (16), we can calculate the difference between the rf frequency and the resonance frequency ω_{mn}

$$|\omega-\omega_{mn}|=\frac{\rho-1}{\rho+1}\Delta\omega\ .$$

Similar considerations were used to analyze approximately the data obtained in quartz.[4,5]

IV. OTHER RESULTS

A. Near resonance with two transitions sharing a common level

In Sec. III we analyzed the case in which the rf frequency was close to one and only one transition frequency. If we consider other possibilities then we obtain more complicated results. The most general case is one in which we consider every term in Eqs. (9) to be significant. In this case we obtain 13 frequency components near every non-negative integral multiple of the rf frequency. Although this very general case is of little practical interest, at least one generalization of the analysis of Sec. II B is important. This is the case when ω is near two frequencies ω_{lm} and ω_{mn}, a case which occurs for the $F=1$ state of muonium and which was encountered in the studies of muonium in quartz reported in a companion paper.[5]

For the case in which ω is close to both ω_{lm} and ω_{mn} the differential equations of Eq. (5) become

$$\frac{da_k}{dt}=0\,,$$

$$\frac{da_l}{dt}=-\frac{i}{2}\Omega_{lm}a_m e^{-i(\omega-\omega_{lm})t}e^{-i\phi}\,,$$

$$\frac{da_m}{dt}=-\frac{i}{2}\Omega^*_{lm}a_l e^{i(\omega-\omega_{lm})t}e^{i\phi}-\frac{i}{2}\Omega_{mn}a_n e^{-i(\omega-\omega_{mn})t}e^{-i\phi}\,,$$

$$\frac{da_n}{dt}=-\frac{i}{2}\Omega^*_{mn}a_m e^{i(\omega-\omega_{mn})t}e^{i\phi}\,.$$

The resulting determinantal eigenvalue equation in terms of the frequencies of a_m is

$$\begin{vmatrix} \omega_m^{(i)}-\omega+\omega_{lm} & \frac{1}{2}\Omega_{lm}e^{-i\phi} & 0 \\ \frac{1}{2}\Omega^*_{lm}e^{i\phi} & \omega_m^{(i)} & \frac{1}{2}\Omega_{mn}e^{-i\phi} \\ 0 & \frac{1}{2}\Omega^*_{mn}e^{i\phi} & \omega_m^{(i)}+\omega-\omega_{mn} \end{vmatrix}=0\,.$$

Having solved this equation, the coefficients of the various oscillatory terms in the $a_i(t)$ can be obtained from 2 of the 3 linear equations and the initial values $a_i(0)$. These can then be used to calculate the components of $\vec{P}(t)$ using Eqs. (6)—(8). Because the eigenvalue equation is cubic, numerical solutions were employed. The results of a calculation which is illustrative are shown in Fig. 4.

In this case there are seven frequency components in the precession of the μ^+ spin polarization. For low rf magnetic fields these are close to the values $3\omega-\omega_{lm}-\omega_{mn}$, $2\omega-\omega_{lm}$, $2\omega-\omega_{mn}$, ω, ω_{lm}, ω_{mn}, and $-\omega+\omega_{lm}+\omega_{mn}$, except when the rf frequency is near ω_{lm}, ω_{mn}, or $\frac{1}{2}(\omega_{lm}+\omega_{mn})$. Near these three values of the rf frequency, the lines which would otherwise cross, avoid each other and the intensities vary so that away from these avoided crossings only the lines near ω_{lm} and ω_{mn} have appreciable intensity. Consequently, when ω is near resonance with either transition, only the five lines predicted in Sec. II B have appreciable intensity. For rf magnetic fields which are large enough so that $|\Omega_{lm}|$ and $|\Omega_{mn}|$ are comparable to $|\omega_{lm}-\omega_{mn}|$, then all seven lines may have appreciable intensity and the avoided crossings are more complex.

In Fig. 4 the DEMUR spectrum for an isotropic muoniumlike center is calculated for a rather large rf magnetic field. When the rf magnetic field is close to resonance with either of the two transitions then a five-line spectrum is observed as predicted by the theory of Sec. II B. The splittings of the three lines near the rf frequency and the two lines near the transition which is not driven are equal, also in

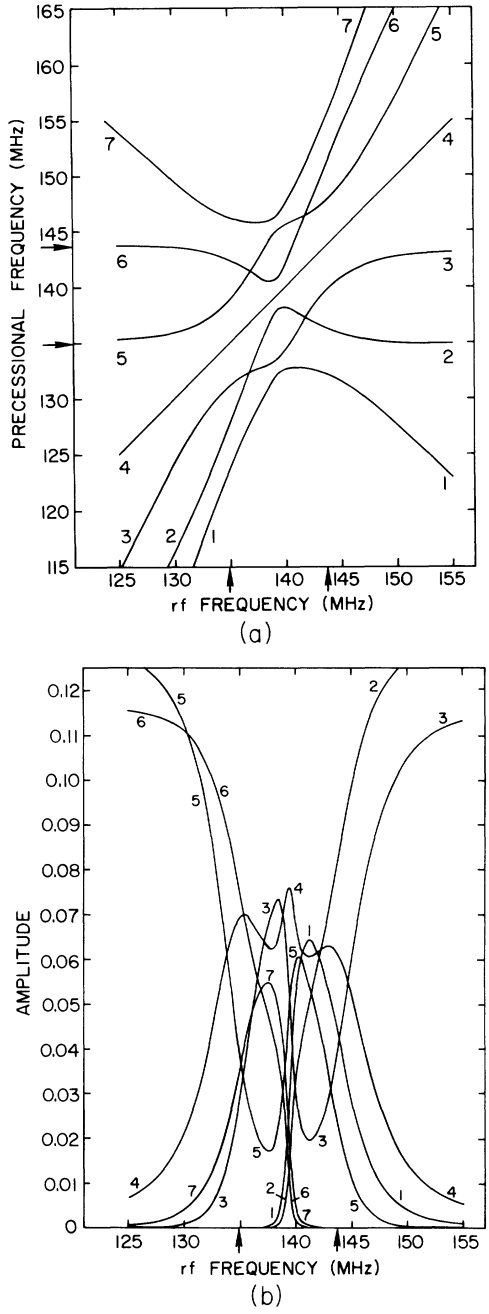

FIG. 4. DEMUR spectrum for muonium when the rf field is large enough to drive both low-frequency transitions. These graphs were made for $g=2$, $A=4500$ MHz, $H_0=100$ G, and $H_1=4$ G. Figure 4(a) is a plot of the actual precessional frequencies versus the frequency of the applied rf field. The two resonance frequencies are shown on both axes by arrows. Figure 4(b) is a plot of the amplitudes of the seven lines shown in Fig. 4(a) against the frequency of the applied rf field. The two resonant frequencies are indicated with arrows. The curves are numbered so as to match those of Fig. 4(a).

agreement with the more elementary theory of Sec. II B. However, there are several differences. When the rf frequency is equal to one of the transition frequencies, the two lines near the other transition frequency are not equally spaced about the other transition frequency. Their mean position is on the opposite side of the undriven transition from the driven one. In addition the amplitudes of these two lines are not equal on resonance and the three lines near the rf frequency do not have a 1:2:1 amplitude ratio on resonance. The minimum splitting of the groups of two and three lines also does not occur on resonance but rather at an rf frequency lower than the lower transition frequency and higher than the higher transition frequency. These effects are somewhat analogous to the Bloch-Siegert shift.[21]

The avoided crossings for rf frequencies near $\frac{1}{2}(\omega_{lm}+\omega_{mn})$ correspond to a two-photon resonance. For rf fields less than or of the order of 1 G, there is very little evidence of this feature, consistent with its two-photon character.

B. DEMUR of a muoniumlike center with nuclear hyperfine structure

The analysis for a muoniumlike center with nuclear hyperfine structure proceeds much like the analysis of Sec. II A except that there are additional terms in the spin Hamiltonian, Eq. (1). Consequently there are more stationary states, so that Eq. (3) for $\Psi(t)$ has more contributions, as do Eqs. (5), the differential equations for the $a_i(t)$. For low-static fields the theory of DEMUR could be very complicated as could the μSR frequency spectrum with no applied rf.

At high-static fields the results are much simpler; provided that the rf magnetic field is not too large, it is reasonable to say that ω is near one and only one EPR frequency and only two μSR frequencies occur. The analysis of Sec. II B is then valid although more stationary states occur.

If we confine our discussion to the case of a single nucleus of spin $\frac{1}{2}$, then there are four strong EPR transitions in high field. When the rf frequency is resonant with one of these four EPR transitions, the two μSR lines will each be split into three lines. Half of the amplitude of each μSR line, that corresponding to a particular nuclear spin state, will be split into two lines as given by Eqs. (18), and the other half will be unaffected. Thus on resonance with random rf phase a symmetric pattern with a 1:2:1 ratio of amplitudes occurs for each μSR line. Off resonance the amplitudes and splittings are both asymmetric. As the nuclear spins or the number of nuclei involved increase, the intensity of the unsplit line increases relative to the two lines which are split. DEMUR would clearly not be simple and easy to see except in the simplest cases of nuclear hyperfine structure.

C. Other magnetic resonance experiments on μ^+ and muonium

There have been numerous experiments first on[22] μ^+ and then on muonium[23] in which magnetic resonance was detected by observations of the changes of the static muon spin polarization along the direction of the applied static field. Such behavior for a muoniumlike center is shown by the z dependence of the static polarization in Eq. (19) and for selected driven transitions of muonium in Eqs. (30) and (31). Since the aim of these magnetic resonance experiments is much different than those of DEMUR, the experimental conditions are quite different, and the analysis which we have used may not always be appropriate. The experiments on muonium measure the magnetic dipole transitions of the muon spin precisely so as to extract accurate values of the muonium hyperfine splitting. They are not designed to use time-differential μSR techniques and thus to obtain the μ^+ spin precessional frequencies. Consequently they do not display the various coherence effects observable in DEMUR nor can one study weak EPR transitions as in DEMUR.

D. Comparison to coherence effects observed in other ways

DEMUR is a technique which works only because of the coherence effects. The intense rf magnetic field drives the system, frequently just one transition, and the state of the system and the polarization vary coherently with the driving field. The splittings, shifts, and amplitude variations which depend on the magnitude and frequency of the rf field are all coherence effects. Without these DEMUR could not be detected.

There are many other kinds of experiments in which coherence effects are observed and there are many papers about magnetic resonance or atomic physics which relate to this subject. Two examples will be discussed which, if combined, illustrate the kinds of effects analyzed in Sec. III A.

In nuclear magnetic resonance experiments at low frequencies and in the earth's field, Béné and his collaborators[24] have observed that in the resonance of spin-$\frac{1}{2}$ nuclei such as protons the response of the system has three frequency components. This is the same as the behavior of $\vec{P}_{43}(t)$ in Eqs. (29) and (30) with the rf frequency near resonance with ω_{43}. A qualitative explanation for this is given in Sec. I.

Coherence effects are also observed in electron nu-

clear double resonance (ENDOR).[25] One form that these experiments take involves high microwave power, i.e., a large rf field driving the EPR transitions. A splitting of the NMR transitions is observed when the frequency of the low-power rf field is near a resonance of the nuclear spins. This behavior is similar to that observed in $\vec{P}_{32}(t)$ in Eq. (29) when the rf frequency is near ω_{43}.

V. CONCLUSION

We have presented a rather general theoretical treatment of DEMUR together with results for two specific cases of interest, muonium and the anomalous muonium centers observed in Si, Ge, and diamond. The theory has been tested in experiments on muonium in quartz and other applications are under study. The results are similar to those for other coherence effects. The special features of μSR have been incorporated into this treatment as has been the absence of observed relaxation in the systems to which the theory has been applied.

ACKNOWLEDGMENTS

The authors have received frequent help and advice from our collaborators S. A. Dodds, R. H. Heffner, M. Leon, J. A. Brown, and K. W. Blazey. This work was supported by the National Science Foundation under Grant No. DMR-79-09223.

---

*Present address: Hewlett-Packard Corp., Palo Alto, CA 94304.

[1]See the papers in Hyperfine Interact. 8, 307-834 (1981).

[2]J. H. Brewer, K. M. Crowe, F. N. Gygax, and A. Schenck, in *Muon Physics,* edited by V. W. Hughes and C. S. Wu (Academic, New York, 1975), Vol. 3, Chap. 7, p. 3.

[3]Preliminary presentations of aspects of this theory were given in Ref. 4 and in T. L. Estle, S. A. Dodds, D. A. Vanderwater, J. A. Brown, R. H. Heffner, and M. Leon, Bull. Am. Phys. Soc. 25, 243 (1980); D. A. Vanderwater, S. A. Dodds, T. L. Estle, J. A. Brown, R. H. Heffner, M. Leon, and D. W. Cooke, Hyperfine Interact. 8, 823 (1981).

[4]J. A. Brown, R. H. Heffner, M. Leon, S. A. Dodds, D. A. Vanderwater, and T. L. Estle, Phys. Rev. Lett. 43, 1751 (1979).

[5]J. A. Brown, R. H. Heffner, M. Leon, S. A. Dodds, T. L. Estle, and D. A. Vanderwater, following paper, Phys. Rev. B 27, 3980 (1983).

[6]J. A. Brown, S. A. Dodds, T. L. Estle, R. H. Heffner, M. Leon, and D. A. Vanderwater, Solid State Commun. 33, 613 (1980).

[7]K. W. Blazey, J. A. Brown, D. W. Cooke, S. A. Dodds, T. L. Estle, R. H. Heffner, M. Leon, and D. A. Vanderwater, Phys. Rev. B 23, 5316 (1981).

[8]C. Boekema, E. Holzschuh, W. Kündig, P. F. Meier, B. D. Patterson, W. Reichart, and K. Rüegg, Hyperfine Interact. 8, 401 (1981).

[9]K. Blum, in *Progress in Atomic Spectroscopy,* edited by W. Hanle and H. Kleinpoppen (Plenum, New York, 1978), Part A, Ch. 2, p. 71.

[10]R. P. Feynman, F. L. Vernon, Jr., and R. W. Hellwarth, J. Appl. Phys. 28, 49 (1957).

[11]B. D. Patterson, A. Hintermann, W. Kündig, P. F. Meier, F. Waldner, H. Graf, E. Recknagel, A. Weidinger, and T. Wichert, Phys. Rev. Lett. 40, 1347 (1978).

[12]E. Holzschuh, H. Graf, E. Recknagel, A. Weidinger, T. Wichert, and P. F. Meier, Phys. Rev. B 20, 4391 (1979).

[13]E. Holzschuh, W. Kündig, P. F. Meier, B. D. Patterson, J. P. F. Sellschop, M. C. Stemmet, and H. Appel, Phys. Rev. A 25, 1272 (1982).

[14]G. E. Pake and T. L. Estle, *The Physical Principles of Electron Paramagnetic Resonance* (Benjamin, Reading, Mass., 1973), p. 98.

[15]The linearly-polarized rf field is often taken to have amplitude $2H_1$ so that the properly rotating component has amplitude H_1. In this paper the amplitude of the field is taken to be H_1.

[16]B. D. Patterson, C. Boekema, and P. F. Meier, Hyperfine Interact. 8, 811 (1981).

[17]This initial wave function must be such that the muon is 100% polarized along the direction of the beam but the electron is unpolarized. This can be done by introducing coordinates describing the electron spin orientation and averaging these when the polarization is later calculated [see Eqs. (24)—(26)].

[18]J. H. Brewer, D. S. Beder, and D. P. Spencer, Phys. Rev. Lett. 42, 808 (1979).

[19]It is conventional to label the stationary states of muonium in order of decreasing energy. Since only the lowest state can be defined uniquely (there is always a higher energy state), in many fields the reverse convention is used. We adopt the latter convention and label states from the lowest up. If level crossings occur the convention will be defined more precisely at that time.

[20]E. Roduner, Hyperfine Interact. 8, 561 (1981).

[21]F. Bloch and A. Siegert, Phys. Rev. 57, 522 (1940).

[22]T. Coffin, R. L. Garwin, S. Penman, and A. M. Sachs, Phys. Rev. 106, 1108 (1957); 109, 973 (1958).

[23]P. A. Thompson, P. Crane, T. Crane, J. J. Amato, V. W. Hughes, G. zu Putlitz, and J. E. Rothberg, Phys. Rev. A 8, 86 (1973); D. Favart, P. M. McIntyre, D. Y. Stowell, V. L. Telegdi, R. De Voe, and R. A. Swanson, *ibid.* 8, 1195 (1973), and references therein.

[24]G. J. Béné, Phys. Rep. 58, 213 (1980).

[25]L. Kevan and L. D. Kispert, *Electron Spin Double Resonance Spectroscopy* (Wiley, New York, 1976), p. 109.